Dicopper(I) Trefoil Knots: Topological and Structural Effects on the Demetalation Rates and Mechanism

Michel Meyer,[†] Anne-Marie Albrecht-Gary,*[,‡] Christiane O. Dietrich-Buchecker,[§] and Jean-Pierre Sauvage*[,§]

Contribution from the Laboratoire de Physico-Chimie Bioinorganique, URA 405 du CNRS, ECPM, 1 rue Blaise Pascal, 67000 Strasbourg, France, and Laboratoire de Chimie Organo-Minérale, URA 422 du CNRS, Faculté de Chimie, Université Louis Pasteur, 4 rue Blaise Pascal, 67000 Strasbourg, France

Received October 28, 1996[⊗]

Abstract: The cyanide-assisted demetalation kinetics of four molecular dicopper(I) trefoil knots, related face-to-face constitutional isomers and of a double-stranded helical knot's precursor, have been investigated by single-wavelength and multiwavelength absorption spectrophotometry in order to gain insight into the particular properties induced by interlacing four 1,10-phenanthroline chelating units. The nonentangled face-to-face and helical dinuclear complexes are demetalated according to a two consecutive, bimolecular rate-limiting step mechanism. In each case, both coordination sites are structurally equivalent and dissociate in an almost statistical way, reflecting weak interactions between them. In contrast, the knotted topology is responsible for a strong coupling as evidenced by the one and two rate-limiting step processes found for the methylene- and phenylene-bridged knots, respectively. This result has been rationalized in terms of molecular rearrangements of the knotted structure following the release of the first copper(I) cation. Hence, the coordination sphere becomes either more accessible to the entering cyanide anion and the mononuclear intermediate dissociates in a fast second step or highly protecting, leading to an inert mononuclear species in the case of the phenylene-bridged knot. The 9 orders of magnitude span of the second-order demetalation rate constants reflects the versatile structural parameters around the copper(I) center. They are primarily affected by the steric hindrance of the substituents in the 2,9-positions of the phenanthroline nuclei and by the topology of the complex. Compared with their face-to-face analogues, the methylene-bridged knots are about 100 times more inert as a result of the helicoidal arrangement of the internal spacer in the core of the molecule. Furthermore, the kinetic parameters are sensitive to even more subtle structural variations, like the length of the internal and external spacers.

Introduction

Molecular knots have been discussed for many years as hypothetical chemical objects.[1−4] They can be defined as a simple closed curve embedded in a 3-dimensional space that does not intersect itself.[5] Hence, all knots are topologically nonplanar. The molecular graph of the trefoil knot, the most simple representative of the family, has three crossings.[6] Thus, the trefoil knot exhibits topological chirality since all three crossing points or nodes are of the same sign: either positive (right-handed enantiomer) or negative (left-handed enantiomer). In 1976, molecular-biology studies afforded the first example of a molecular knot: extracts of single-stranded DNA from *Escherichia coli* were shown to contain a mixture of the left- and right-handed trefoil knots.[7] Since, numerous examples of both single- and double-stranded knotted DNA have been described.[8] Specific enzymes, called topoisomerases or gyrases, are responsible for the entwining of DNA by carrying out the breakage of either one or both strands, interlacing and finally reconnecting them.[9] Subsequently, Liang and Mislow uncovered the presence of knotted loops formed from polypeptide chain segments restrained by cysteine disulfide bridges and/or cofactors in two proteins, ascorbate oxidase and human lactoferrin.[10]

However, it is only recently that the first molecular knots have been synthesized and characterized.[11] One approach is reminiscent of the naturally occurring DNA knots and utilizes synthetic polynucleotides.[12] Our strategy relies on the three-dimensional template effect of two copper(I) centers able to induce the formation of a dinuclear helical complex, precursor

* To whom correspondence should be addressed.
[†] Present address: Department of Chemistry, University of California, Berkeley, CA.
[‡] URA 405 du CNRS.
[§] URA 422 du CNRS.
[⊗] Abstract published in *Advance ACS Abstracts,* April 15, 1997.

(1) Frisch, H. L.; Wasserman, E. J. *J. Am. Chem. Soc.* **1961**, *83*, 3789.
(2) Schill, G. *Catenanes, Rotaxanes and Knots*; Academic Press: New York, 1971.
(3) (a) Walba, D. M. In *Chemical Applications of Topology and Graph Theory*; King, R. B., Ed.; Elsevier: New York, 1983. (b) Walba, D. M. *Tetrahedron* **1985**, *41*, 3161.
(4) Van Gulick, N. *New J. Chem.* **1993**, *17*, 619.
(5) Crowell, R. H.; Fox, R. H. *Introduction to Knot Theory*; Springer-Verlag: New York, 1963.
(6) Schücker, T. *New J. Chem.* **1993**, *17*, 655.
(7) Liu, L. F.; Depew, R. E.; Wang, J. C. *J. Mol. Biol.* **1976**, *106*, 439.
(8) (a) Mizuuchi, K.; Fisher, L. M.; O'Dea, M. H.; Gellert, M. *Proc. Natl. Acad. Sci. U.S.A.* **1980**, *77*, 1487. (b) Dean, F. B.; Stasiak, A.; Koller, T.; Cozzarelli, N. R. *J. Biol. Chem.* **1985**, *260*, 4975. (c) Griffith, J. D.; Nash, H. A. *Proc. Natl. Acad. Sci. U.S.A.* **1985**, *82*, 3124. Wasserman, S. A.; Cozzarelli, N. R. *Science* **1986**, *232*, 951.
(9) (a) Tse, Y.-C.; Wang, J. C. *Cell* **1980**, *22*, 269. (b) Gellert, M. *Annu. Rev. Biochem.* **1981**, *50*, 879. (c) Wang, J. C. *Annu. Rev. Biochem.* **1985**, *54*, 665. (d) Uemura, T.; Yanagida, M. *EMBO J.* **1984**, *3*, 1737. (e) Wang, J. C. *J. Biol. Chem.* **1991**, *266*, 6659.
(10) (a) Liang, C.; Mislow, K. *J. Am. Chem. Soc.* **1994**, *116*, 11189. (b) Liang, C.; Mislow, K. *J. Am. Chem. Soc.* **1995**, *117*, 4201.
(11) (a) Dietrich-Buchecker, C. O.; Sauvage, J.-P. *Bioorganic Chemistry Frontiers*; Dugas, H., Ed.; Springer-Verlag: Berlin, 1991; Vol. 2, p 146. (b) Dietrich-Buchecker, C. O.; Sauvage, J.-P. *Bull. Soc. Chim. Fr.* **1992**, *129*, 113. (c) Amabilino, D. B.; Stoddart, J. F. *Chem. Rev.* **1995**, *95*, 2725.
(12) (a) Mueller, J. E.; Du, S. M.; Seeman, N. C. *J. Am. Chem. Soc.* **1991**, *113*, 6306. (b) Du, S. M.; Seeman, N. C. *J. Am. Chem. Soc.* **1992**, *114*, 9652. (c) Seeman, N. C.; Chen, J.; Du, S. M.; Mueller, J. E.; Zhang, Y.; Fu, T.-J.; Wang, Y.; Wang, H.; Zhang, S. *New J. Chem.* **1993**, *17*, 739.

S0002-7863(96)03737-7 CCC: $14.00

of the trefoil knot.[13−17] Although the preparative yields for these compounds were generally modest (0.5−8%), reasonable amounts of the dicopper(I) complexes could be obtained. The X-ray structure of an 86-membered and 84-membered knotted ring have been reported[14,15,17] as well as the electrochemical and photophysical properties[16] of some dicopper(I) knots and related face-to-face isomers containing covalently distinct macrocyclic subunits. Recently, the synthetic procedure was dramatically improved by introducing 1,3-phenylene spacers between the chelates, allowing high-yield preparation of the corresponding dicopper(I) trefoil knot.[18,19]

The present paper deals with cyanide-induced demetalation kinetic studies. The chemical formulaes of the various copper(I) complexes considered in this work are presented in Figure 1, whereas their overall demetalation reactions are represented in Schemes 1−3. The cyanide-assisted demetalation mechanism and the corresponding kinetic parameters, obtained for the dinuclear copper(I) knots $Cu_2(K\text{-}84)^{2+}$, $Cu_2(K\text{-}86)^{2+}$, $Cu_2(K\text{-}90)^{2+}$, and $Cu_2(K\text{-}Ph\text{-}84)^{2+}$, for the related face-to-face constitutional isomers $Cu_2(M\text{-}43)_2{}^{2+}$ and $Cu_2(M\text{-}45)_2{}^{2+}$, and for the double-stranded helical complex $Cu_2(map\text{-}Ph\text{-}map)_2{}^{2+}$, the precursor of the $Cu_2(K\text{-}Ph\text{-}84)^{2+}$ knot, are discussed in terms of *topological and topographical* (i.e., geometrical) effects. The kinetic properties of the various complexes investigated have been revealed to be very sensitive to both factors, in a way reminiscent of the catenate structure.[20−22] They lead to very large differences in demetalation rates. The most spectacular effects are found within the molecular knots family, for which decomplexation rate constants span over 7 orders of magnitude.

Results

Prior to the kinetic investigations, absorption spectrophotometric studies of the different copper(I) complexes and the free ligands liberated by the reaction with cyanide were carried out under the same experimental conditions. As an example, the electronic spectra of the dinuclear complex $Cu_2(K\text{-}86)^{2+}$ and of the demetalated knot K-86 are presented in Figure 2 over the 250−650 nm range. Upon decomplexation, the intense ($\epsilon \approx 10^5$ M^{-1} cm^{-1}) ligand-centered $\pi \rightarrow \pi^*$ and $n \rightarrow \pi^*$ transitions showing up below 380 nm undergo a hyperchromic effect, whereas the broad and less intense metal-to-ligand charge-transfer (MLCT) bands disappear in the visible region (Table 1). A detailed interpretation of these MLCT bands has recently been reported[16] based on the assignment proposed for the bis(2,9-dimethyl-1,10-phenanthroline)copper(I) complex.[23] In agreement with a previous study carried out in pure methylene chloride,[16] very similar absorption spectra were recorded for

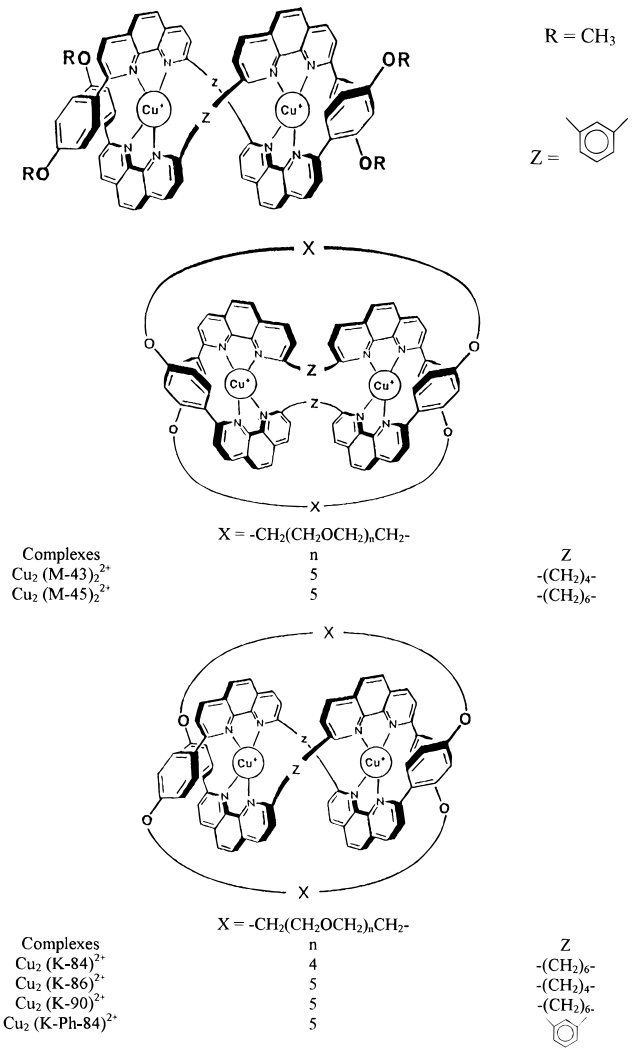

Figure 1. Chemical formulas of various mononuclear and dinuclear copper(I) complexes considered in this paper. Each knot is represented by the letter K accompanied by the overall number of atoms included in the cycle. The face-to-face complexes contain two monocycles (letter M), the number of atoms in each ring being also indicated. It can be noted that each knot has a face-to-face counterpart, except $Cu_2(K\text{-}86)^{2+}$ and $Cu_2(K\text{-}Ph\text{-}84)^{2+}$.

the methylene-bridged knots, the face-to-face analogs, and the mononuclear model compound $Cu(Memap)_2{}^+$ (Memap = 2-(*p*-anisyl)-9-methyl-1,10-phenanthroline), suggesting comparable coordination environments in spite of very different topologies. Noteworthy, the two dicopper(I) complexes containing 1,3-phenylene bridges, $Cu_2(K\text{-}Ph\text{-}84)^{2+}$ and $Cu_2(map\text{-}Ph\text{-}map)_2{}^{2+}$, display identical absorption properties, but they are markedly contrasted with those of the other complexes as evidenced by the brick-red to purple color change. The extinction coefficients determined at the maximum of the charge-transfer band are presented in Table 1 for all complexes considered in this work.

The overall demetalation reactions by cyanide are illustrated in Schemes 1−3 and can be expressed for the nonknotted and knotted dinuclear complexes by eqs 1 and 2, respectively.

$$Cu_2L_2{}^{2+} + 8CN^- \rightarrow 2L + 2\ Cu(CN)_4{}^{3-} \qquad (1)$$

$$Cu_2K^{2+} + 8CN^- \rightarrow K + 2\ Cu(CN)_4{}^{3-} \qquad (2)$$

The dissociation process of the double-helical complex $Cu_2(map\text{-}Ph\text{-}map)_2{}^{2+}$ and of both face-to-face complexes studied under pseudo-first-order conditions by absorption spectropho-

(13) Dietrich-Buchecker, C. O.; Sauvage, J.-P. *Angew. Chem., Int. Ed. Engl.* **1989**, *28*, 189.
(14) Dietrich-Buchecker, C. O.; Guilhem, J.; Pascard, C.; Sauvage, J.-P. *Angew. Chem., Int. Ed. Engl.* **1990**, *29*, 1154.
(15) Dietrich-Buchecker, C. O.; Sauvage, J.-P.; Kintzinger, J.-P.; Maltèse, P.; Pascard, C.; Guilhem, J. *New J. Chem.* **1992**, *16*, 931.
(16) Dietrich-Buchecker, C. O.; Nierengarten, J.-F.; Sauvage, J.-P.; Armaroli, N.; Balzani, V.; De Cola, L. *J. Am. Chem. Soc.* **1993**, *115*, 11237.
(17) Albrecht-Gary, A.-M.; Dietrich-Buchecker, C. O.; Guilhem, J.; Meyer, M.; Pascard, C.; Sauvage, J.-P. *Recl. Trav. Chim. Pays-Bas* **1993**, *112*, 427.
(18) Dietrich-Buchecker, C. O.; Sauvage, J.-P.; De Cian, A.; Fisher, J. *J. Chem. Soc., Chem. Commun.* **1994**, 2231.
(19) Dietrich-Buchecker, C. O.; Sauvage, J.-P.; Armaroli, N.; Ceroni, P.; Balzani, V. *Angew. Chem., Int. Ed. Engl.* **1996**, *35*, 1119.
(20) Dietrich-Buchecker, C. O.; Sauvage, J.-P.; Kern, J.-M. *J. Am. Chem. Soc.* **1984**, *106*, 3043.
(21) Albrecht-Gary, A.-M.; Saad, Z.; Dietrich-Buchecker, C. O.; Sauvage, J.-P. *J. Am. Chem. Soc.* **1985**, *107*, 3205.
(22) Albrecht-Gary, A.-M.; Dietrich-Buchecker, C. O.; Saad, Z.; Sauvage, J.-P. *J. Am. Chem. Soc.* **1988**, *110*, 1467.
(23) Everly, R. M.; Mc Millin, D. R. *J. Phys. Chem.* **1992**, *95*, 9071.

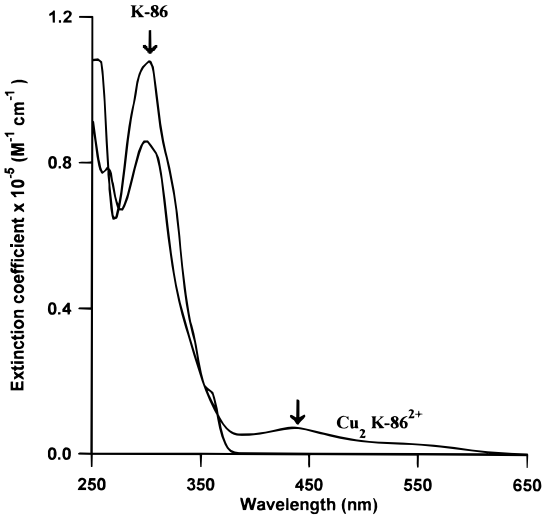

Figure 2. Visible absorption spectra of $Cu_2(K\text{-}86)^{2+}$ and of the free ligand K-86: solvent $CH_3CN/CH_2Cl_2/H_2O$, 80/15/5 v/v; $I = 0.1$ (n-$Bu)_4N^+CF_3SO_3^-$; $T = 25$ °C. The arrow indicates the wavelength chosen for kinetic measurements.

tometry shows a double-exponential variation of the absorbance with time. A typical kinetic trace recorded with a stopped-flow spectrophotometer for $Cu_2(M\text{-}43)_2^{2+}$ is shown in Figure 3a. The two pseudo-first-order rate constants k^f_{obs} and k^s_{obs} determined for the faster and slower steps, respectively, increase linearly with increasing cyanide concentration as depicted in Figure 4a for $Cu_2(M\text{-}43)_2^{2+}$.

The second-order rate constants k^f_{CN} and k^s_{CN} corresponding to the slope of the lines are collected in Table 2. For the slower dissociation step of complexes $Cu_2(M\text{-}43)_2^{2+}$ and $Cu_2(M\text{-}45)_2^{2+}$, ordinates at the origin were found to be significantly different from zero according to the statistical t-test and the test described by Hamilton:[24,25] $k_D = 5.0 \pm 0.3$ and 0.4 ± 0.2 s^{-1}, respectively. For a spectrophotometric detection and a reaction sequence involving two consecutive irreversible steps (eq 3), the extinction coefficient of the intermediate I is expressed by eq 4, with a^s the spectrophotometric amplitude of the slower step and $[Cu_2L_2^{2+}]_{tot}$ the analytical concentration of the complex, assuming the products are not absorbing.[26] The extinction

$$Cu_2L_2^{2+} \xrightarrow{k^f_{obs}} I \xrightarrow{k^s_{obs}} 2L + 2Cu^+ \quad (3)$$

$$\epsilon_I = \frac{(k^f_{obs} - k^s_{obs})}{k^f_{obs}[Cu_2L_2^{2+}]_{tot}} a^s \quad (4)$$

coefficients of the intermediate calculated for $Cu_2(map\text{-}Ph\text{-}map)_2^{2+}$, $Cu_2(M\text{-}43)_2^{2+}$, and $Cu_2(M\text{-}45)_2^{2+}$ at the maximum of the charge-transfer band are 1300 ± 100 ($\lambda = 520$ nm), 3100 ± 200 ($\lambda = 434$ nm), and 2900 ± 400 ($\lambda = 440$ nm) M^{-1} cm^{-1}, respectively. They correspond approximately to half of the extinction coefficients determined for the corresponding dinuclear complexes (Table 1). In order to characterize further the intermediate species, time-resolved absorption spectra in the 380−650 nm range were recorded for both $Cu_2(map\text{-}Ph\text{-}map)_2^{2+}$ and $Cu_2(M\text{-}45)_2^{2+}$ complexes (Figure 5). Owing to factor analysis, the spectrophotometric data could be described in both cases by three distinct absorbing species. A satisfactory least-squares fit of the apparent rate constants and extinction coefficients was only obtained with the reaction scheme given by eq 3. The calculated absorption spectra shown in Figure 6 of the reactants and products are identical to those measured at equilibrium, whereas the intermediate species I can unambiguously be assigned to a mononuclear complex. $Cu_2(M\text{-}45)_2^{2+}$ and $Cu(M\text{-}45)_2^+$ exhibit similar spectral profiles with a 2-fold lower intensity for the former, suggesting that the coordination environment in both compounds has substantially the same symmetry. A noticeably different situation is encountered in the case of $Cu_2(map\text{-}Ph\text{-}map)_2^{2+}$ as evidenced by very different spectral features of the mono- and dinuclear complexes.

The experimental rate law together with the spectrophotometric results supports the following mechanism, where k_D is an intrinsic first-order rate constant related to the dissociation of the mononuclear intermediate CuL_2^+ formed at the end of the faster step[21] and k^f_{CN} and k^s_{CN} represent the second-order rate constants relative to the faster and slower steps, respectively:

$$Cu_2L_2^{2+} + CN^- \xrightarrow{k^f_{obs}} CuCu(CN)L_2^+$$

$$CuCu(CN)_x L_2^{2-x} + CN^- \xrightarrow{fast} CuCu(CN)_{x+1} L_2^{1-x} \quad (1 \le x \le 2)$$

$$CuCu(CN)_3 L_2^- + CN^- \xrightarrow{fast} CuL_2^+ + Cu(CN)_4^{3-}$$

$$CuL_2^+ + CN^- \xrightarrow{k^s_{obs}} Cu(CN)L_2 \quad (5)$$

$$CuL_2^+ \xrightarrow{k_D} 2L + Cu^+$$

$$Cu(CN)_x L_2^{1-x} + CN^- \xrightarrow{fast} Cu(CN)_{x+1} L_2^{-x} \quad (1 \le x \le 2)$$

$$Cu(CN)_3 L_2^{2-} + CN^- \xrightarrow{fast} 2L + Cu(CN)_4^{3-}$$

$$Cu^+ + 4CN^- \xrightarrow{fast} Cu(CN)_4^{3-}$$

This proposed ligand exchange mechanism leads to the following rate equations:

$$-\frac{d[Cu_2L_2^{2+}]}{dt} = k^f_{obs}[Cu_2L_2^{2+}] = k^f_{CN}[CN^-]_{tot}[Cu_2L_2^{2+}] \quad (6)$$

$$\frac{d[CuL_2^+]}{dt} = k^f_{obs}[Cu_2L_2^{2+}] - k^s_{obs}[CuL_2^+] = k^f_{CN}[CN^-]_{tot}[Cu_2L_2^{2+}] - \{k_D + k^s_{CN}[CN^-]_{tot}\}[CuL_2^+] \quad (7)$$

$$\frac{d[Cu(I)]}{dt} = k^s_{obs}[CuL_2^+] = \{k_D + k^s_{CN}[CN^-]_{tot}\}[CuL_2^+] \quad (8)$$

The demetalation reaction of the three knots possessing internal methylenic chains ($Cu_2(K\text{-}84)^{2+}$, $Cu_2(K\text{-}86)^{2+}$, and $Cu_2(K\text{-}90)^{2+}$) proceeds in a single rate-limiting step in excess of cyanide, as shown by the monoexponential absorbance decay in Figure 3b for $Cu_2(K\text{-}86)^{2+}$. The variations of the pseudo-first-order rate constants with the total concentration of cyanide

(24) Commissariat à l'Energie Atomique. *Statistique Appliquée à l'Exploitation des Mesures*; Masson: Paris, 1979.
(25) Hamilton, W. C. *Statistics in Physical Science*; Ronald Press: New York, 1964.
(26) Wilkins, R. G. *Kinetics and Mechanism of Reactions of Transition Metal Complexes*; VCH: Weinheim, 1991; pp 16−23.

Table 1. Spectrophotometric Properties of the Various Complexes Studied[a]

complex	λ_{max} (nm)	ϵ (M^{-1} cm^{-1})	complex	λ_{max} (nm)	ϵ (M^{-1} cm^{-1})
$Cu(Memap)_2^{+}$ [b]	440 ± 2	4400 ± 100	$Cu_2(K\text{-}84)^{2+}$	430 ± 2	6100 ± 100
$Cu(dap)_2^{+}$ [b]	430 ± 2	2500 ± 100	$Cu_2(K\text{-}86)^{2+}$	436 ± 2	6200 ± 100
$Cu_2(map\text{-}Ph\text{-}map)_2^{2+}$	524 ± 2	2800 ± 100	$Cu_2(K\text{-}90)^{2+}$	430 ± 2	6200 ± 100
$Cu_2(M\text{-}43)_2^{2+}$	434 ± 2	6600 ± 100	$Cu_2(K\text{-}Ph\text{-}84)^{2+}$	520 ± 2	3200 ± 100
$Cu_2(M\text{-}45)_2^{2+}$	440 ± 2	6300 ± 100			

[a] Solvent $CH_3CN/CH_2Cl_2/H_2O$, 80/15/5 v/v; I = 0.1 $(n\text{-}Bu)_4N^+CF_3SO_3^-$; T = 25 °C. [b] Reference 29.

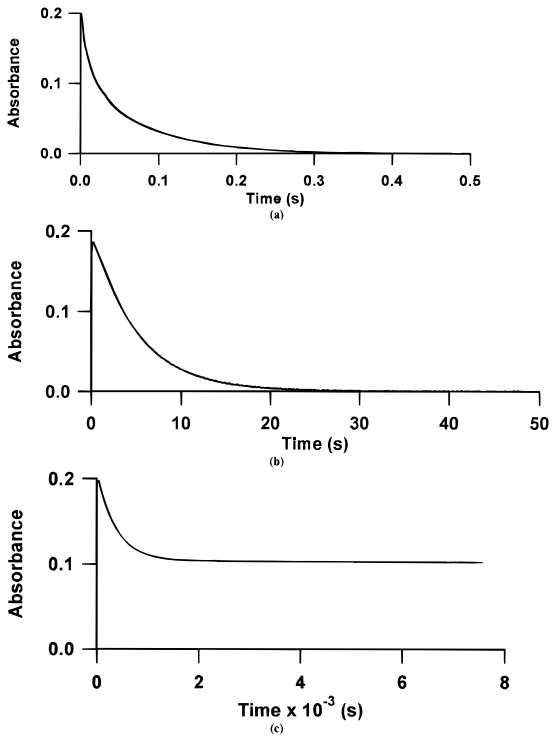

Figure 3. Experimental kinetic traces obtained for the demetalation of (a) $Cu_2(M\text{-}43)_2^{2+}$, (b) $Cu_2(K\text{-}86)^{2+}$, and (c) $Cu_2(K\text{-}Ph\text{-}84)^{2+}$: solvent $CH_3CN/CH_2Cl_2/H_2O$, 80/15/5 v/v; I = 0.1 $(n\text{-}Bu)_4N^+CF_3SO_3^-$; T = 25 °C; (a) $[Cu_2(M\text{-}43)_2^{2+}] = 3.24 \times 10^{-5}$ M, $[CN^-] = 1.80 \times 10^{-3}$ M, λ = 434 nm; (b) $[Cu_2(K\text{-}86)^{2+}] = 2.73 \times 10^{-5}$ M, $[CN^-] = 1.89 \times 10^{-3}$ M, λ = 436 nm; (c) $[Cu_2(K\text{-}Ph\text{-}84)^{2+}] = 7.08 \times 10^{-5}$ M, $[CN^-] = 2.58 \times 10^{-2}$ M, λ = 524 nm.

are linear without any significant intercept at the origin (Figure 4b). The corresponding rate law, valid for the three knotted complexes considered, is given by eq 9, and the values of the second-order rate constants k_{CN} are included in Table 2.

$$v = -\frac{d[Cu_2K^{2+}]}{dt} = k_{obs}[Cu_2K^{2+}] = k_{CN}[CN^-]_{tot}[Cu_2K^{2+}] \quad (9)$$

In addition to different spectroscopic properties, the behavior of the phenylene-bridged knot $Cu_2(K\text{-}Ph\text{-}84)^{2+}$ in the presence of cyanide markedly contrasts with the demetalation scheme observed for the aliphatic counterparts. $Cu_2(K\text{-}Ph\text{-}84)^{2+}$ displays a much more inert character; hence, its dissociation has been studied by classical absorption spectrophotometry at the wavelength corresponding to the maximum of the MLCT band (λ = 524 nm). Two rate-limiting steps, well-resolved in time, are observed (Figure 3c) in contrast to the one rate-limiting step found for the three aliphatic knots. The faster absorbance decay is monoexponential and takes place in the hour range. The associated amplitude is close to half the total amplitude. The pseudo-first-order rate constants for this step were obtained by nonlinear least-squares adjustment. Subsequently, the signal continues to decrease in an extremely slow way: after 4−5 days only 20% of the remaining amplitude is lost. Decomposition of the cyanide becomes significant over that period of time and prevents following the reaction to completion. Hence, the absorbance decrease with time is almost linear,[27] and the corresponding apparent rate constants were estimated from the slope of the least-squares line adjusted to the experimental data points. Similarly to all the other complexes, the kinetic parameters related to both the faster and the slower steps increase linearly with the analytical cyanide concentration (Figure 4c, Table 2). The rate law for the phenylene-bridged knot is thus identical to the one described previously for its precursor, the double-helical $Cu_2(map\text{-}Ph\text{-}map)_2^{2+}$ complex, and is given by eqs 6−8. The spectrum of the mononuclear intermediate $Cu(K\text{-}Ph\text{-}84)^+$ recorded at the end of the faster step differs markedly from that of the dinuclear $Cu_2(K\text{-}Ph\text{-}84)^{2+}$ knot (Figure 7): the absorption maxima for the higher and the lower energy transitions are red-shifted by ca. 10 and 30 nm, respectively.

Discussion

All the bimolecular rate constants k_{CN} determined in the present work and related to the helical precursor, the face-to-face complexes, and the various knots are presented in Table 2. For the sake of comparison, the corresponding kinetic parameters determined under the same experimental conditions for one unsymmetrical, $Cu(Memap)_2^+$, and one symmetrical, $Cu(dap)_2^+$ (dap = 2,9-di-(*p*-anisyl-1,10-phenanthroline), copper(I) bischelate and for the 30-membered ring catenate, Cucat-30^+, are also included.[29]

The 9 orders of magnitude span of the bimolecular rate constants reflects the highly versatile topography, compactness, and accessibility to the nucleophile scavenger encountered at each metal center.[21,28] In terms of topology, the number of crossings in the molecular graph can be considered as an important factor which reflects the entanglement level of the system. For the face-to-face complexes formed by two independent macrocycles and for the double helix, the number of crossings is equal to zero. Indeed, the molecular graph of a double helix is open and thus is identical, from a topological point of view, to two parallel lines if the connectivity of all atoms remains the same in both arrangements. The entanglement level increases from the [2]catenane structure with two crossings per molecule to the trefoil knot with three crossings per molecule. Therefore, the kinetic properties of the dinuclear helix, the face-to-face complexes, and the knots will be discussed in terms both of topology (i.e., entanglement) and of topography (i.e., spatial arrangement).

The nonknotted face-to-face analogs show a classical behavior for nonentangled dinuclear complexes. Similarly to threaded systems formed by a bisphenanthroline string threaded in two

(27) The error introduced by approximating the first 20% amplitude loss of a monoexponential decay by the tangent at the origin is less than 3%.

(28) Chambron, J.-C.; Dietrich-Buchecker, C. O.; Nierengarten, J.-F.; Sauvage, J.-P.; Solladié, N.; Albrecht-Gary, A.-M.; Meyer, M. *New J. Chem.* **1995**, *19*, 409.

(29) Meyer, M.; Albrecht-Gary, A.-M.; Dietrich-Buchecker, C. O.; Sauvage, J.-P. Manuscript in preparation.

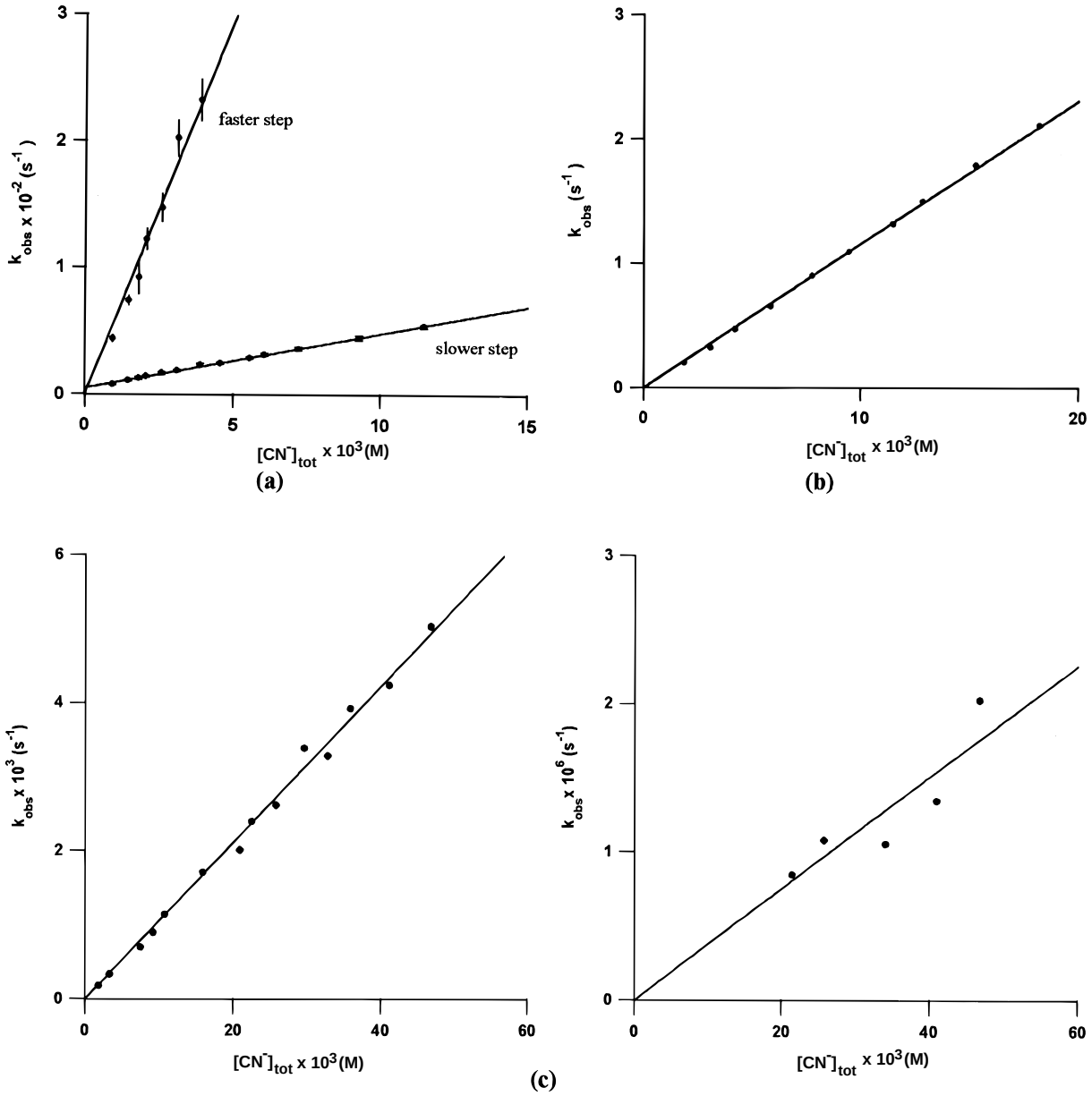

Figure 4. Pseudo-first-order rate constant k_{obs} as a function of cyanide concentration for (a) $Cu_2(M\text{-}43)_2^{2+}$, (b) $Cu_2(K\text{-}86)^{2+}$, and (c) $Cu_2(K\text{-}Ph\text{-}84)^2$: solvent $CH_3CN/CH_2Cl_2/H_2O$, 80/15/5 v/v; $I = 0.1$ (n-Bu)$_4N^+CF_3SO_3^-$; $T = 25$ °C; (a) $[Cu_2(M\text{-}43)_2^{2+}] = 3.24 \times 10^{-5}$ M; (b) $[Cu_2(K\text{-}86)^{2+}] = 2.73 \times 10^{-5}$ M; (c) $[Cu_2(K\text{-}Ph\text{-}84)^{2+}] = 7.08 \times 10^{-5}$ M.

independent coordinating macrocycles by the templating copper(I) cations,[28] the demetalation reaction proceeds in two bimolecular steps as depicted in Scheme 1. This result is intuitively expected from a topological point of view. Since the degree of entanglement is equal to zero, only limited conformational changes have to take place during the decomplexation process.

The second-order rate constants corresponding to the first demetalation step of $Cu_2(M\text{-}43)_2^{2+}$ ($k_{CN} = 5.8 \times 10^4$ M^{-1} s^{-1}) and $Cu_2(M\text{-}45)_2^{2+}$ ($k_{CN} = 1.3 \times 10^4$ M^{-1} s^{-1}) are very similar to the bimolecular rate constant obtained for the mononuclear model compound $Cu(Memap)_2^+$ ($k_{CN} = 2.4 \times 10^4$ M^{-1} s^{-1}). Since these parameters reflect structural factors like the steric hindrance around the metal center and in agreement with the similar spectroscopic properties (Table 1), it might be expected that the coordination geometry of the copper(I) ions contained in these complexes is almost the same. In the absence of crystallographic information for $Cu(Memap)_2^+$, stability constants and kinetic measurements support the idea of a highly distorted pseudotetrahedral coordination geometry due to stacking interactions between one phenanthroline core and the phenyl group attached to the other phenanthroline chelate.[29] This assumption is also consistent with the X-ray structure of the face-to-face complex $Cu_2(M\text{-}43)_2^{2+}$.[15] The coordination polyhedra around each copper center show an open face (140.5°) oriented toward its neighbor, whereas the accessibility of the opposite face to the entering cyanide anion is strongly hindered by the almost planar (dihedral angle of 15°) overlapping of the phenyl substituents of one M-43 ring and the phenanthroline nucleus belonging to the facing macrocycle. The similar spectroscopic properties and dissociation rate constants of $Cu(Memap)_2^+$ and $Cu_2(M\text{-}43)_2^{2+}$ indicate that the external polyoxyethylenic chains which tether both coordination centers in the latter species, do not affect their geometry and accessibility.

Compared to $Cu_2(M\text{-}43)_2^{2+}$, the complex $Cu_2(M\text{-}45)_2^{2+}$ dissociates about 2 times more slowly. Longer methylenic bridges between both phenanthroline nuclei in the larger macrocycle induce a slightly better shielding against the nucleophile. For both face-to-face complexes, the ratio of the faster over the slower step rate constants ranges between 5 and 10, and is thus close to the statistical value. This result, in

Table 2. Cyanide-Assisted Second-Order Dissociation Rate Constants[a]

mononuclear complex	one-step mechanism $k_{CN} \pm \sigma$ ($M^{-1}\,s^{-1}$)
$Cu(Memap)_2^{+}$ [b]	$(2.37 \pm 0.02) \times 10^4$
$Cu(dap)_2^{+}$ [b]	8.8 ± 0.4
Cucat-30^{+} [b]	0.479 ± 0.004

	two-step mechanism	
	$k^f_{CN} \pm \sigma$ ($M^{-1}\,s^{-1}$)	$k^s_{CN} \pm \sigma$ ($M^{-1}\,s^{-1}$)
double-stranded helix		
$Cu_2(map\text{-}Ph\text{-}map)_2^{2+}$	2.22 ± 0.04	0.323 ± 0.004
face-to-face complex		
$Cu_2(M\text{-}43)_2^{2+}$	$(5.83 \pm 0.09) \times 10^4$	$(4.29 \pm 0.06) \times 10^3$
$Cu_2(M\text{-}45)_2^{2+}$	$(1.30 \pm 0.03) \times 10^4$	$(2.87 \pm 0.06) \times 10^3$

knot	one-step mechanism $k_{CN} \pm \sigma$ ($M^{-1}\,s^{-1}$)
$Cu_2(K\text{-}84)^{2+}$	5.59 ± 0.04
$Cu_2(K\text{-}86)^{2+}$	115.5 ± 0.6
$Cu_2(K\text{-}90)^{2+}$	44.6 ± 0.5

	two-step mechanism	
knot	$k^f_{CN} \pm \sigma$ ($M^{-1}\,s^{-1}$)	$k^s_{CN} \pm \sigma$ ($M^{-1}\,s^{-1}$)
$Cu_2(K\text{-}Ph\text{-}84)^{2+}$	0.105 ± 0.002	(3.8 ± 0.3) x 10^{-5}

[a] Solvent $CH_3CN/CH_2Cl_2/H_2O$, 80/15/5 v/v; $I = 0.1$ (n-Bu)$_4N^+$-$CF_3SO_3^-$; $T = 25$ °C. [b] Reference 29.

agreement with structural[15] and electrochemical[16] studies, indicates that both centers are nearly equivalent in the dinuclear complex and that the coordination environment remains substantially unchanged in the mononuclear intermediate. This is also evidenced by the identical shape but twice less intense charge-transfer absorption band of $Cu(M\text{-}43)_2^+$ compared to the dinuclear $Cu_2(M\text{-}43)_2^{2+}$ parent compound.

The most striking result obtained for the methylene-bridged knotted analogs is the apparent single-step decomplexation mechanism. Therefore, *the rate limiting step of dissociation of the first copper(I) cation has to be followed by a faster decomplexation process for the second one*. The reaction pathway is presented in the Scheme 2. This observation clearly shows that the kinetic properties of a given copper(I) center depend significantly on the second metal center. Demetalation of the first coordination site makes the second metal more accessible to external attacks and thus facilitates its removal. In fact, it has been shown that, in the completely demetalated systems, a profound molecular rearrangement has taken place via *reptation* motions, to afford a new structure with the phenanthroline chelates located at the periphery of the molecule.[15]

In spite of chemically identical and structurally similar coordination polyhedra,[15] the single rate-limiting dissociation step of $Cu_2(K\text{-}86)^{2+}$ and $Cu_2(K\text{-}90)^{2+}$ is, respectively, 3 and 2 orders of magnitude slower than the first and second demetalation steps of the corresponding face-to-face analogs. This observation can be rationalized in terms of structure. In the face-to-face situation, the tetramethylenic links located between the two coordination sites of $Cu_2(M\text{-}43)_2^{2+}$ are extended along the Cu−Cu direction and lie in two almost parallel planes, whereas they form a double helix in the knotted $Cu_2(K\text{-}86)^{2+}$ complex.[15] A longer metal−metal distance is measured (7.94 Å for $Cu_2(M\text{-}43)_2^{2+}$) in comparison with the knot $Cu_2(K\text{-}86)^{2+}$ (6.3 Å), leading to less compact and more accessible copper(I) complexes.

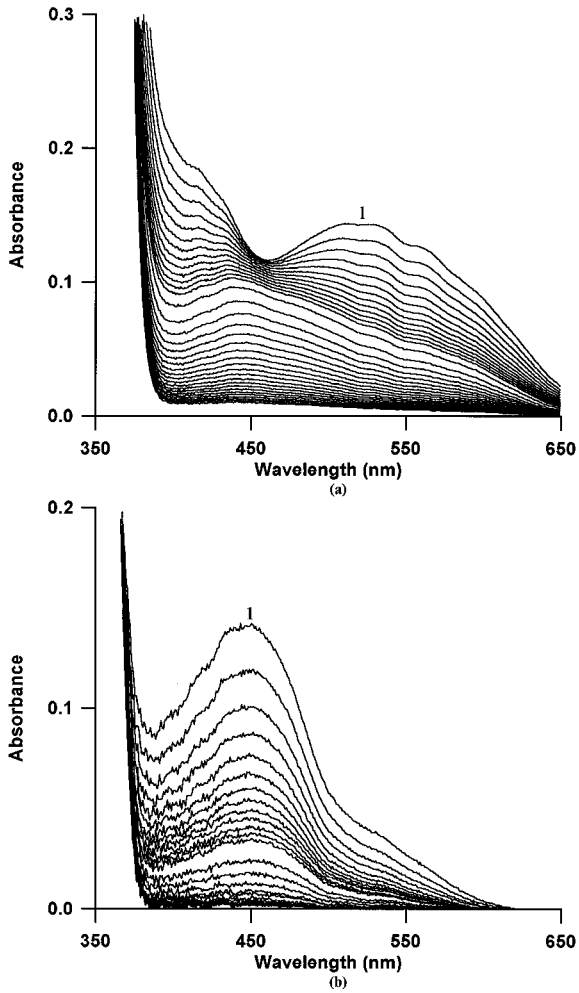

Figure 5. Time-resolved absorption spectra recorded for the cyanide-assisted dissociation of (a) $Cu_2(map\text{-}Ph\text{-}map)_2^{2+}$ and (b) $Cu_2(M\text{-}45)_2^{2+}$: solvent $CH_3CN/CH_2Cl_2/H_2O$, 80/15/5 v/v; $I = 0.1$ (n-Bu)$_4N^+$-$CF_3SO_3^-$; $T = 25$ °C; (a) $[Cu_2(map\text{-}Ph\text{-}map)_2^{2+}] = 6.3 \times 10^{-5}$ M, $[CN^-] = 4.07 \times 10^{-2}$ M, $t_1 = 0.44$ s and then one spectrum every 1.76 s, $t_{14} = 29.64$ s and then one spectrum every 1.76 s; (b) $[Cu_2(M\text{-}45)_2^{2+}] = 3.3 \times 10^{-5}$ M, $[CN^-] = 9.76 \times 10^{-4}$ M, $t_1 = 0.015$ s and then one spectrum every 0.03 s, $t_{13} = 0.42$ s and then one spectrum every 0.12 s.

Along the series, the second-order demetalation rate constants for the three knots vary significantly, by more than 1 order of magnitude, although their chemical structures may appear relatively similar to one another.[15,17] In agreement with X-ray diffraction studies, the more compact system, $Cu_2(K\text{-}84)^{2+}$, is the slowest to demetalate ($k_{CN} = 5.59\ M^{-1}\,s^{-1}$). Compared to $Cu_2(K\text{-}90)^{2+}$, shortening the external polyoxyethylenic chains by one $-OCH_2CH_2-$ unit while keeping the length of the internal tether constant (hexamethylenic chain) induces an 8-fold decrease of the demetalation rate constant k_{CN} which reflects the tighter copper(I) core of $Cu_2(K\text{-}84)^{2+}$. Considering the two hexaoxyethylenic-bridged knots, $Cu_2(K\text{-}86)^{2+}$ dissociates three times faster than the larger counterpart, $Cu_2(K\text{-}90)^{2+}$. Although no crystal structure for $Cu_2(K\text{-}90)^{2+}$ is available, it appears that the double helix formed with the longer $-(CH_2)_6-$ fragments offers a better shielding around both copper(I) centers than the shorter $-(CH_2)_4-$ fragment. Hexamethylenic linkers allow more freedom in the relative position of both copper(I) subunits which leads to a more pronounced twist angle between them in $Cu_2(K\text{-}84)^{2+}$ (70°) compared with $Cu_2(K\text{-}86)^{2+}$ (30°).[15,17] This

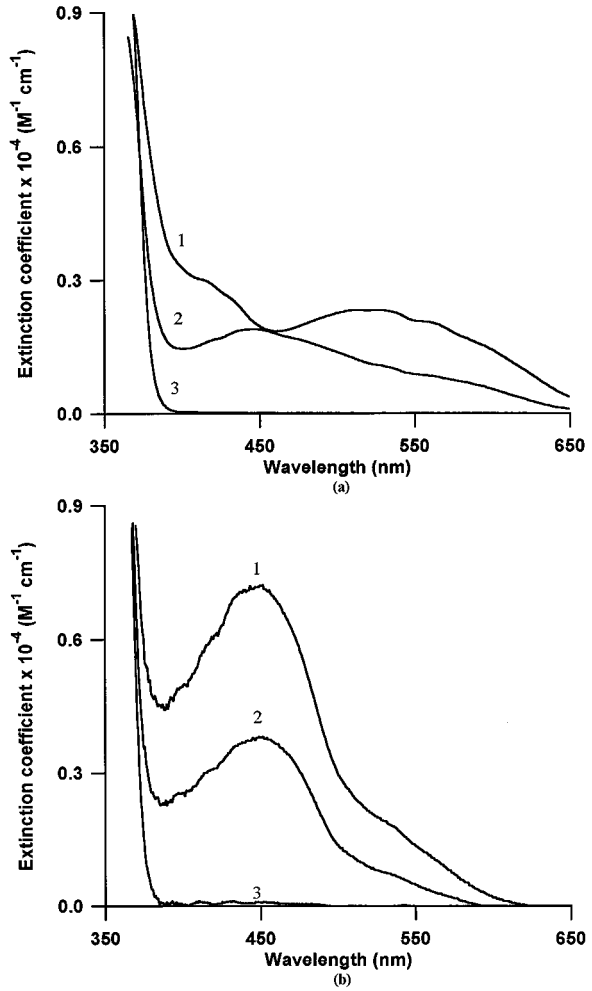

Figure 6. Calculated spectra of the reactants (1), the intermediate (2), and the products (3) of the demetalation of (a) $Cu_2(map\text{-}Ph\text{-}map)_2^{2+}$ and (b) $Cu_2(M\text{-}45)_2^{2+}$: solvent $CH_3CN/CH_2Cl_2/H_2O$, 80/15/5 v/v; I = 0.1 $(n\text{-}Bu)_4N^+CF_3SO_3^-$; T = 25 °C.

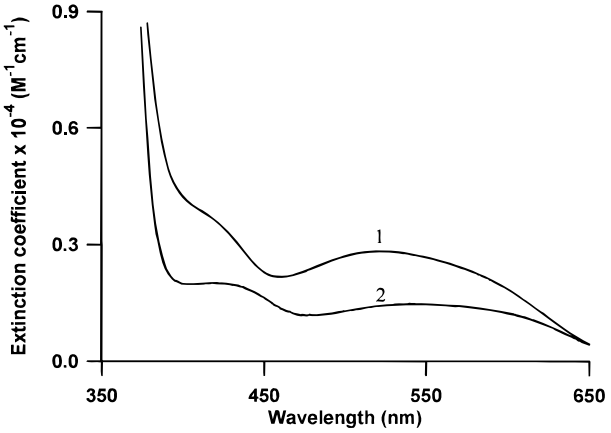

Figure 7. Absorption spectra of the dinuclear $Cu_2(K\text{-}Ph\text{-}84)^{2+}$ (1) and the mononuclear $Cu(K\text{-}Ph\text{-}84)^+$ (2) knots: solvent: $CH_3CN/CH_2Cl_2/H_2O$, 80/15/5 v/v; I = 0.1 $(n\text{-}Bu)_4N^+CF_3SO_3^-$; T = 25 °C.

results in a 0.7 Å shorter metal−metal distance and in a more compact shape of the more wound double-helical core. However, the shorter $-CH_2(CH_2OCH_2)_4CH_2-$ connectors in $Cu_2(K\text{-}84)^{2+}$ may also be in part responsible for the more compact geometry of the 84-membered knot.

It is also of interest to compare our kinetic results with electrochemical and photophysical properties of the dicopper(I) knotted complexes.[16] The relevant data are collected in Table 3. Noteworthy, the redox potential of $Cu_2(K\text{-}84)^{2+}$ in acetonitrile[16] has been found to be surprisingly high ($E°$ = 0.75 V vs SCE), the potential recorded for the 86-membered knotted cycle being about 140 mV lower. This observation is in perfect agreement with our kinetic results: the tightest and most rigid system $Cu_2(K\text{-}84)^{2+}$ is formed by $-(CH_2)_6-$ links, ensuring efficient shielding of the metal centers and by $-CH_2(CH_2OCH_2)_4CH_2-$ chains being too short to allow an easy distortion of the pseudotetrahedral coordination geometry toward a square-planar geometry, the preferential geometry of four-coordinated copper(II). The inertness of $Cu_2(K\text{-}84)^{2+}$ is also reflected by its highest metal-to-ligand charge-transfer (MLCT) excited-state lifetime.[16] Interestingly, the bimolecular demetalation rate constants which reflect the copper(I) accessibility to cyanide in the ground state parallel the excited-state lifetimes which are related to the protecting capability of the ligand toward luminescence quenching interactions in the excited state.

Replacing the central aliphatic spacers between two phenanthroline units by 1,3-phenylene groups induces severe modifications of the electronic and kinetic properties. Both the phenylene-bridged knot, $Cu_2(K\text{-}Ph\text{-}84)^{2+}$, and its helical precursor, $Cu_2(map\text{-}Ph\text{-}map)_2^{2+}$, are decomplexed in two rate-limiting steps. Such a mechanism is expected in the case of the precursor (Scheme 2), since its entanglement level equals zero. The second-order rate constants related to the faster and slower steps are in a ratio of about 7. Thus, both coordination sites in the double helix can be considered as nearly equivalent from a kinetic point of view, as previously found for the face-to-face complexes, although electrochemical measurements revealed

Scheme 1

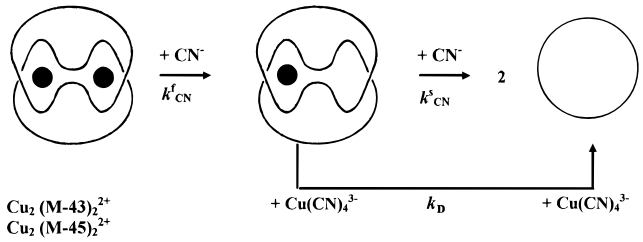

Scheme 2

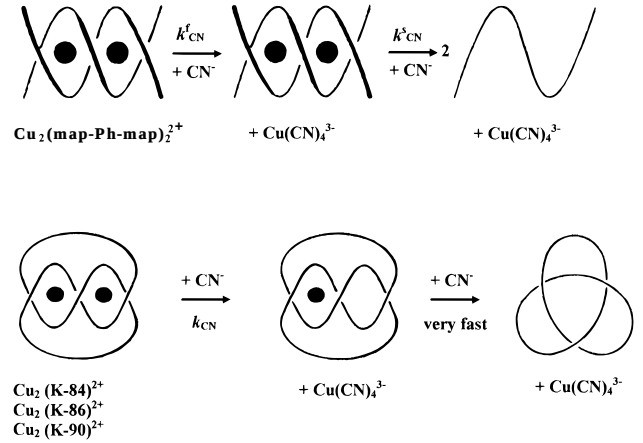

Table 3. Kinetic, Electrochemical,[16] and Photophysical[16] Properties of Dinuclear Copper(I) Knots

complex	k_{CN} [a] ($M^{-1}s^{-1}$)	$E°$ [b] (V vs SCE)	τ [c] (ns)
$Cu_2(K\text{-}86)^{2+}$	115.5	0.61	154
$Cu_2(K\text{-}90)^{2+}$	44.6		174
$Cu_2(K\text{-}84)^{2+}$	5.59	0.75	208

[a] Solvent $CH_3CN/CH_2Cl_2/H_2O$, 80/15/5 v/v; I = 0.1 $(n\text{-}Bu)_4N^+CF_3SO_3^-$; T = 25 °C. [b] Cyclic-voltammetry measurements in CH_3CN; I = 0.1 $LiClO_4$; oxidation on Pt; scan rate 100 mV s^{-1}. [c] Excited-state lifetimes in deaerated CH_2Cl_2 solutions; T = 25 °C.

Scheme 3

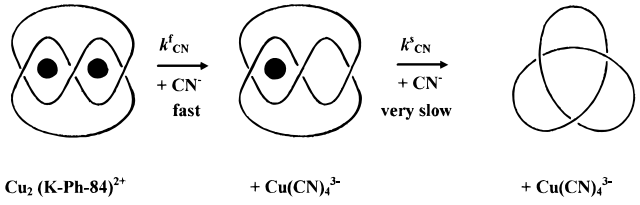

strong electrostatic interactions between the two metals as a consequence of the short Cu−Cu distance (4.76 Å) compared with the 7.94 Å distance in Cu_2(M-43)$^{2+}$.[18]

The two rate-limiting steps observed for Cu_2(K-Ph-84)$^{2+}$ (Scheme 3) clearly indicate that the apparent dissociation mechanism (i.e., the number of rate-limiting steps) is not governed by the topologic factors alone, as it could be inferred at first sight from the study of the methylene-bridged knots. Obviously, the structural factor plays an important role as evidenced by the two limiting situations encountered: the dissociation of the second site relative to the first can occur either faster, as observed in the case of the three methylene-bridged knots, or much more slowly in the case of Cu_2(K-Ph-84)$^{2+}$, leading to an inert mononuclear complex. In contrast to the helical and the face-to-face molecular architectures for which both copper(I) cations are kinetically quasi-equivalent, the coordination sites are strongly coupled in the knotted topology. Our observations evidence that the structural and electronic perturbations arising from the release of the first cation are efficiently transmitted to the second site. As a consequence of the tight entanglement of the coordinates, a conformational change of the organic backbone has to take place, leading to a different topography of the coordination polyhedron in the mononuclear intermediate. Indeed, X-ray structural studies performed on the free catenand cat-30 and its copper(I) complex, Cucat-30$^+$,[30] have clearly shown that both 2,9-diphenyl-1,10-phenanthroline fragments are a long distance apart in the free ligand whereas they are entwined by coordination to the central copper cation in the complex. Kinetic studies have further evidenced the gliding motion responsible for the disentangling of the chelating units followed by the complete disengagement of the molecule while both rings remain interlocked.[21] Solvation of the uncoordinated phenanthroline nuclei which pushes them as far as possible away, may contribute to the driving force of such a molecular rearrangement. The kinetic results can thus be rationalized by assuming that the metal becomes more accessible in the methylene-bridged series whereas an increased protecting environment around the remaining copper cation arises for the phenylene derivative. The distinct spectral features of Cu(K-Ph-84)$^+$ and Cu_2(K-Ph-84)$^{2+}$ (Figure 7) further support this interpretation. A CPK model and recently an X-ray structure[31] show that Cu(K-Ph-84)$^+$ continues to display a helical conformation in spite of its free site. The release of one cation reduces to some extent the strain, thus allowing the remaining cation to interact more strongly with both coordinated phenanthroline nuclei. This tight packing of the monometallic core can also be observed in the proton NMR spectrum. Compared with the dinuclear species, the aromatic hydrogen atoms belonging to both the coordinated and uncoordinated phenanthroline moieties are significantly upfield shifted.

Since both substituents in the 2 and 9 positions of the chelating units exhibit similar bulkiness, the second-order rate constants reported in Table 2 for Cu_2(K-Ph-84)$^{2+}$ and its precursor are of the same order of magnitude as those determined for the symmetric and entwined Cu(dap)$_2^+$ complex or the 30-membered catenate Cucat-30$^+$. The double-stranded helicoidal precursor releases its first copper(I) cation about 20 times faster than Cu_2(K-Ph-84)$^{2+}$, and its complete demetalation is still 3 times faster *than the first Cu(I) release from* Cu_2*(K-Ph-84)*$^{2+}$, reflecting the steric protection of the outer polyoxyethylenic linkers. In addition, the steric hindrance introduced by these chains most probably contributes to slow down demetalation, since they may hinder the rearrangement and gliding process. This hindering effect which leads to different topographies of Cu(K-Ph-84)$^+$ and Cu(map-Ph-map)$_2^+$ is illustrated by their different spectrophotometric properties, while the parent dinuclear complexes exhibit almost identical spectral profiles (Figures 6 and 7). Interestingly, the replacement of the internal methylenic spacers by 1,3-phenylene units decreases the bimolecular rate constants only by a factor of 60 in the case of the two 84-membered knots, whereas nonsymmetric 2,9-disubstitution of the phenanthroline chelate reduces the inertness by 3 orders of magnitude when Cu(Memap)$_2^+$ and Cu(dap)$_2^+$ are compared. However, the 4 orders of magnitude difference between the bimolecular rate constants relative to the faster step and the slower step, gained by dissociating one site of Cu_2(K-Ph-84)$^{2+}$, constitutes a remarkable confirmation of the mechanism outlined in Scheme 3 for the knotted topology. The extraordinary inertness of Cu(K-Ph-84)$^+$ combined with its unusual spectroscopic properties ultimately assesses the rearrangement or motion of the entire molecular knot after the first site becomes unoccupied. The harsh conditions employed to yield the free ligand on a preparative scale further exemplify the view of an almost inaccessible metal center sitting inside an organic cavity. Complete demetalation occurred after Cu(K-Ph-84)$^+$ was allowed to reflux for 24 h in acetonitrile with a 1000-fold excess of potassium cyanide. Interestingly, the remetalation reaction of the mononuclear complex seems much easier, allowing the preparation of the first heterodinuclear knots.[19]

In conclusion, the kinetic data have pointed out the importance of both topological and geometrical effects in the knotted structure. Whereas the coordination sites for the nonentangled dinuclear complexes behave in an almost statistical way, the knotted topology drastically increases the interactions between the two copper(I) cations. If strong interactions can be expected between the phenanthroline subunits with rigid linkers like the 1,3-phenylene moieties, the more flexible alkyl chains also ensure a remarkably efficient coupling of both sites as a consequence of their helical arrangement in the core of the knot. As a consequence of the entangled nature of the trefoil knots, a molecular rearrangement of the entire structure takes place after the release of the first copper(I) cation. Depending on the steric features of the internal spacers, the resulting mononuclear intermediate may offer either a less (methylene spacers) or a more (phenylene spacers) protecting environment around the remaining cation which leads to a one or a two rate-limiting step mechanism, respectively. Hence, the number of rate-limiting steps reflects the topography of the mononuclear knots. The shielding of the metal centers by the organic backbone is highly dependent on the bulkiness of the internal spacers and on the topology, as shown by a widerange span of the decomplexation rates. For a given entanglement level, aryl spacers between the phenanthroline nuclei lead to several orders of magnitude more inert complexes compared with alkyl chains. The helicoidal arrangement of the internal connectors in the knotted topology offers a much more efficient protection toward the cyanide attack than a linear one. Furthermore, the kinetic

(30) Cesario, M.; Dietrich-Buchecker, C. O.; Guilhem, J.; Pascard, C.; Sauvage, J.-P. *J. Chem. Soc., Chem Commun.* **1985**, 244.

(31) Dietrich-Buchecker, C. O.; Sauvage, J.-P.; De Cian, A.; Fisher, J. To be published.

parameters are sensitive to even more subtle structural variations, like the length of the internal and external spacers.

Experimental Section

All the ligands and their tetrafluoroborate or hexafluorophosphate copper(I) complexes used in the present study were obtained following previously described procedures.[16,18] The decomplexation reactions were studied in a manner analogous to that adopted for copper(I) catenates.[21] The demetalating agent, tetraethylammonium cyanide (Fluka, purum), was used in a mixed homogeneous solvent: acetonitrile (Merck, Uvasol)/methylene chloride (Merck, Uvasol)/deionized and argon-saturated water in the proportions 80/15/5 v/v. It was chosen in order to solubilize both reactants and products of the various decomplexation reactions. The ionic strength was adjusted to 0.1 with tetrabutylammonium trifluoromethanesulfonate (Fluka, puriss. p.a. electrochemical grade) and the temperature maintained constant at 25.0 ± 0.1 °C. The decomplexing agent was always in large excess (at least 10 times) compared to the concentrations of the copper(I) complexes, in order to obtain pseudo-first-order conditions.

Except for Cu_2(K-Ph-84)$^{2+}$ studied by classical absorption spectrophotometry using 1 cm quartz cells (Helma) and an Uvikon 860 (Kontron) spectrophotometer, a fast mixing device was necessary to carry out the kinetic measurements. The fixed wavelength chosen was that of the absorption maximum of the MLCT band. A Durrum-Gibson D-110 stopped-flow spectrophotometer interfaced to a Tandon microcomputer or an Applied Photophysics DX17MV instrument was used. The kinetic data were processed on line with commercial software based on Marquardt[32] or Simplex[33] algorithms. The pseudo-first-order rate constants thus derived are included in the Supporting Information. The second-order rate constants were calculated by nonweighted linear regression and are given together with their corresponding standard deviation. Time-resolved absorption spectra were collected on a hand-driven injection unit equipped with a rapid-scan TIDAS 16 (J&M GmbH) diode array spectrophotometer. The multiwavelength data sets were decomposed into their principal components, and subsequently the rate constants and extinction coefficients were adjusted to the reduced data sets by nonlinear least-squares analysis with the SPECFIT program.[34]

Acknowledgment. We thank J&M GmbH (Aalen, Germany) for making the diode array spectrophotometric equipment available and assisting us with its use. This work has been supported by the Centre National de la Recherche Scientifique (CNRS). M.M. thanks the CNRS and the Conseil Regional d'Alsace for a Ph.D. fellowship.

Supporting Information Available: Tables of the pseudo-first-order dissociation rate constants for Cu_2(map-Ph-map)$_2^{2+}$, Cu_2(M-43)$_2^{2+}$, Cu_2(M-45)$_2^{2+}$, Cu_2(K-84)$^{2+}$, Cu_2(K-86)$^{2+}$, Cu_2(K-90)$^{2+}$, and Cu_2(K-Ph-84)$^{2+}$ (3 pages). See any current masthead page for ordering and Internet access instructions.

JA963737Q

(32) Applied Photophysics Ltd., Leatherhead, U.K., 1992.
(33) Bio-logic Co., Echirolles, France, 1991.
(34) Spectrum Software Associates, Chapel Hill, NC, 1994.